

## CHAPTER V

### GROWTH, STRUCTURAL, ELECTRICAL, MECHANICAL AND NONLINEAR OPTICAL STUDIES OF CREATININIUM 5-SULFOSALICYLATE CRYSTAL

#### 5.1 INTRODUCTION

Organic NLO optical materials are captivate a huge deal of interest due to their high nonlinearity and quick response in electro-optic modulation, optical computing, optical memory and terahertz generation and frequency mixing, etc. above the inorganic materials (Badan et al 1993, Chemla et al 1987). Basically, organic compounds contain high delocalised  $\pi$ -electrons and additional electron donor and electron acceptor on opposite sides of the molecules. From these kinds of molecular units, the molecules tend to be highly polarized, which is the root for high nonlinearity in organic compounds. In the past few decades, the third order nonlinear optical materials had less investigations compared to second order nonlinear optical materials.

In the present context, the researchers are focussing on the third order nonlinear materials due to their requirements in photonic fields. Especially, the third order nonlinear optical materials are investigated for their efficient optical switching behaviour (Prasad et al 1991, Somac et al 2003). This is one of the reasons to design a molecule with higher order nonlinearity

and also it may incorporate them with devices for optical signal processing applications (Natarajan et al 1996, Hameed et al 2003).

The slow evaporation solution growth technique is extensively used for the growth of organic compounds to acquire quality single crystals. Thirumurugan et al (2017) grown Creatininium L-tartrate (CTM) single crystal and reported that CTM crystallizes into orthorhombic crystal system with  $P2_12_12_1$  space group. From UV-Visible studies, the CTM crystal showed the lower cut-off wavelength at 249 nm, and good optical transmittance. Creatininium succinate (CS) was grown by Thirumurugan et al (2015) and found that CS crystal belongs to orthorhombic crystal system with space group  $F2dd$ . The second harmonic efficiency of CS was found to be 1.2 times that of KDP.

Creatininium 4-nitrobenzoate (C4NB) was synthesised and the crystal refinement was made for the grown crystal. C4NB crystallizes into orthorhombic crystal system with  $P2_12_12_1$  space group. The SHG activity was found to be 4.6 times that of KDP (Thirumurugan et al 2017).

The crystal refinement of Creatininium phosphate, Bis (creatininium) 3-nitrophthalate monohydrate, Creatininium hydrogen oxalate monohydrate, creatininium nitrate was reported by Sindhusa et al (2017), Thayanithi et al (2016), Asath Bahadur et al (2007), Berrah et al (2005) respectively.

2-Amino-1-methyl-4-oxo-4, 5-dihydro-1H-imidazol-3-ium 3-carboxy-4-hydroxybenzenesulfonate monohydrate crystal structure was reported by Malarkodi et al (2017).

Marjanovic et al (2010) investigated the anilinium 5-sulfosalicylate synthesized by slow addition of aniline (9 g) to the solution of SSA dehydrate (25 g) in propan-2-ol (50 g) under stirring. Anilinium 5-sulfosalicylate was characterized by FTIR and NMR and thermogravimetric analysis (TGA) techniques. The ANI-SSA material was thermally stable upto 240°C.

The semi-organic Calcium 5-Sulfosalicylate was grown by slow evaporation method (Shalini et al 2017). It was observed that the crystal crystallizes into monoclinic with space group  $P_1n_1$ . The nonlinear optical property of CA5SS was found to be about 0.7 times that of KDP. The laser damage threshold value for CA5SS crystal was found to be  $7.48 \times 10^9$  GW/cm<sup>2</sup>.

Sodium 5-sulfosalicylate dihydrate and sodium [triaqua (5-sulfosalicylato) copper (II)] 2 hemihydrate were synthesized and structure refinement investigation was reported by Marzotto et al (2001).

In the present investigation, the creatinium 5-sulfosalicylate (C5SS) possesses centrosymmetric nature, due to this reason it can be motivated to investigate the third order nonlinear susceptibility ( $\chi^3$ ). The synthesis and bulk growth of creatinium 5-sulfosalicylate single crystal

from aqueous solution have been performed based on the solubility measurement. The grown crystal was characterized by single crystal X-ray diffraction, spectral, thermal, UV-Vis, Photoluminescence, laser damage threshold, dielectric, mechanical and Z-scan measurements and results are inferred.

## **5.2 EXPERIMENTAL**

### **5.2.1 Material Synthesis**

High pure creatinine ( $C_4 H_7 N_3 O$ ) and 5-sulfosalicylic acid ( $C_7 H_6 O_6 S$ ) in stoichiometric ratio were taken to synthesis creatininium 5-sulfosalicylate (C5SS) compound and it is shown in Fig.5.1. Initially, the measured amount of 5-sulfosalicylic acid dissolved in deionized water and appropriate amount of creatinine was slowly added into the solution. The solution was continuously stirred to obtain homogeneous state and the solution was allowed for evaporation using a CT bath. The nucleation stage was occurred in the period of 25 days and C5SS salt was collected at the bottom of the beaker. The purity of the synthesized product was further increased by repeated recrystallization. Then, the growth solution was filtered using high quality filter paper for further purification. The filtered solution was kept at CT bath at  $35^{\circ}C$  with an accuracy of  $\pm 0.01^{\circ}C$ . The evaporation rate of the solution was controlled by covering pinhole laminated sheet.

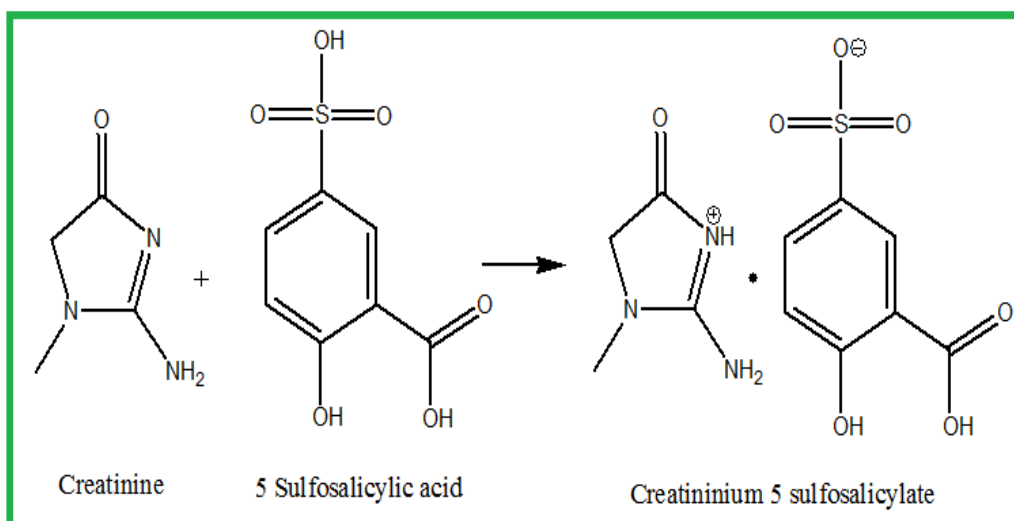


**Fig.5.1 Material synthesis scheme for C5SS compound**

### 5.2.2 Solubility Studies

The solubility study was carried out by using a CT bath with an accuracy  $\pm 0.01^\circ\text{C}$ . Figure 5.2 shows the solubility curve of C5SS compound. Initially, C5SS salt was added into the deionized water solvent and solution was stirred for 6 hr to get the saturation at  $35^\circ\text{C}$ . After reaching the homogeneous state, 10 ml of saturated C5SS solution was taken out, this is allowed to dry in the petri dish. The dried C5SS salt were collected and weighed. It was found to be 34 g at  $35^\circ\text{C}$ . The same procedure was repeated for different temperatures such as 40, 45, 50 and  $55^\circ\text{C}$ . The title compound has a positive temperature gradient which is applicable for slow evaporation growth method.

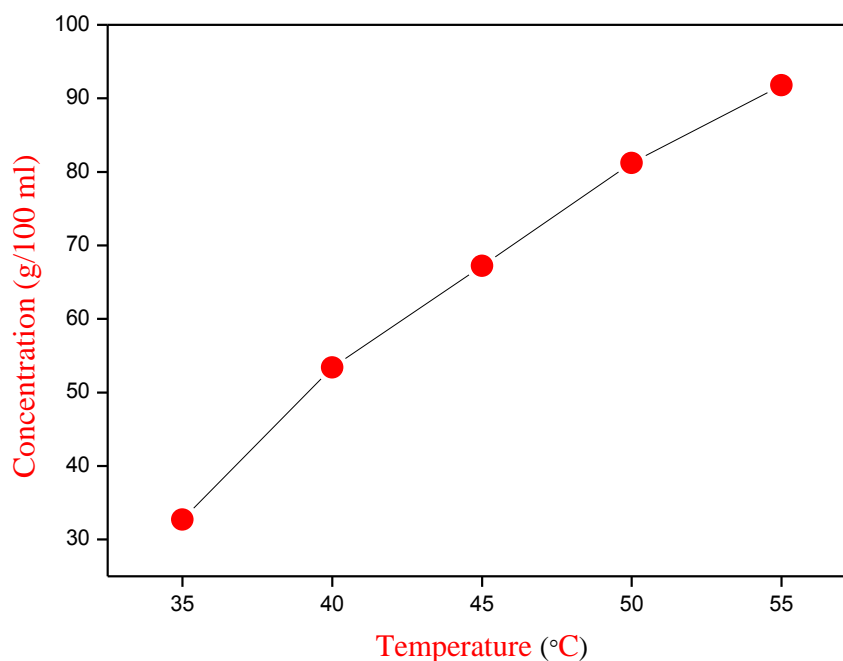


**Fig. 5.2 Solubility of C5SS in water solvent**

### **5.2.3 Crystal Growth and Morphology**

Single crystal of creatinium 5-sulfosalicylate (C5SS) was grown by dissolving the purified salt in the deionized water. The growth solution was stirred continuously for about 6 hr to achieve the homogeneous saturated solution at 35°C. Then, the growth solution was filtered using Whatman filter papers. The beaker containing the solution was closed with a perforated polythene sheet and kept in a CT bath (35°C) with an accuracy of  $\pm 0.01^\circ\text{C}$ . The saturated solution of C5SS salt was prepared at 35°C. The saturated solution yielded good optical quality C5SS single crystal in a period of 25 days and it was collected for characterization. The photograph of grown C5SS single crystal with dimension of 6 x 6 x 2 mm<sup>3</sup> is shown in

Fig.5.3(a). X-ray goniometry was used to identify the crystal planes and morphology of the crystal was drawn by using WinX morph programme. The well developed C5SS crystal was subjected to morphology studies (Fig.5.3(b)), which reveals the prominent hkl growth planes (0 1 1), (-1 1 1), (1 1 -1) and (0 1 0).

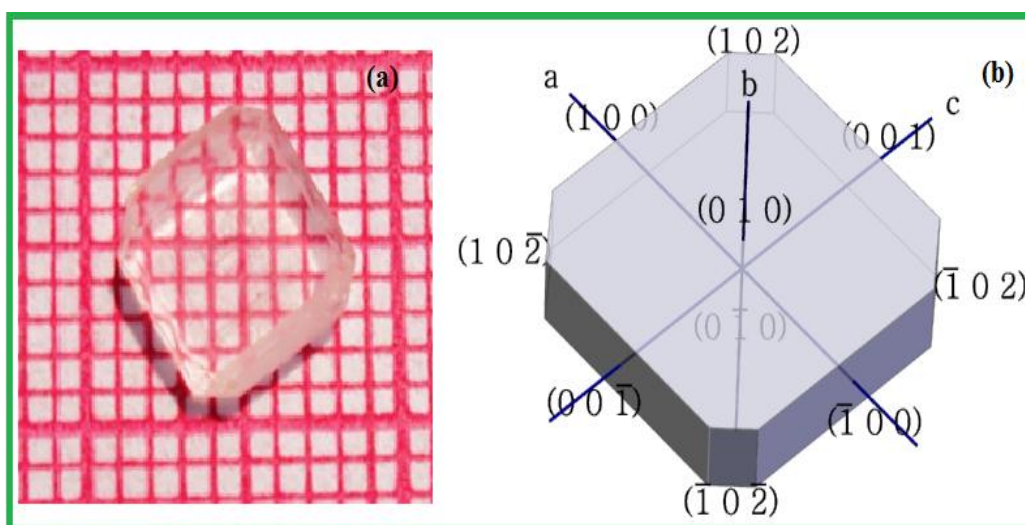


**Fig.5.3 (a) Photograph of as-grown C5SS crystal and (b) Morphology of C5SS crystal**

### 5.3 RESULTS AND DISCUSSION

#### 5.3.1 Single Crystal and Powder X-ray Diffraction Studies

By using BRUKER KAPPA AXS II single crystal X-ray diffractometer with graphite monochromated  $\text{MoK}_\alpha$  radiation ( $\lambda=0.71073 \text{ \AA}$ ) at 293 K, single crystal X-ray diffraction study was performed for the creatininium 5-sulfosalicylate crystal. It crystallizes in monoclinic crystal

system with space group  $P2_1/c$  which belongs to the centrosymmetric crystal structure. The calculated cell parameters are  $a = 7.246 \text{ \AA}$ ,  $b = 13.094 \text{ \AA}$ ,  $c = 15.560 \text{ \AA}$ ,  $\alpha = \gamma = 90^\circ$ ,  $\beta = 94.384^\circ$ ,  $V = 1451.7 \text{ \AA}^3$  and  $Z=4$ . The crystallographic data for structure analysis of the title compound is listed in Table 5.1.

Creatine is extracted from several kinds of muscle and it is endogenously synthesized by the liver and pancreas in humans (Greenhaff et al 1993, Walker et al 1979). We report herein the synthesis and the crystal structure of the title molecular salt (Fig. 5.4). Its geometric parameters agree well with reported data (Thayanithi et al 2016, Jahubar Ali et al 2011). The title compound contains a disordered creatinium cation, with site occupancies of 0.771 (3) for the major component (C2A/N1A/C5A/N4A/C3A/O6A) and 0.229 (3) for minor component (C2B/N1B/C5B/N4B/C3B/O6B), a 5-sulfosalicylate anion and a water molecule in the asymmetric unit. The cation is protonated at the imidazole N atom and the anion is deprotonated at the sulfonic acid group. The benzene ring (C1–C6) is orthogonal to the major [dihedral angle of  $89.7 (2)^\circ$ ] and minor [dihedral angle of  $88.3 (8)^\circ$ ] components of the five-membered rings. In the asymmetric unit, an intra ionic O—H...O hydrogen bond generates an S(6) graph-set motif (Fig. 5.5). In the crystal, an N—H...O hydrogen bond links the anions and cations, generating an  $R_2^2(8)$  ring-motif. The water molecule links adjacent anions

through O—H . . . O hydrogen bonds (Table 5.2 and Fig. 5.5). Weak C—H . . . O contacts (Fig. 5.5 and Table 5.2) link the components into a two-dimensional network parallel to (001).

Powder X-ray diffraction is foremost implement for the study of crystalline materials. The powder X-ray diffraction pattern of C5SS crystal was recorded in the  $2\theta$  range from  $10^{\circ}$  to  $40^{\circ}$  using  $\text{CuK}\alpha$  radiation of wavelength  $1.5406 \text{ \AA}$  as shown in Fig.5.6. The occurrence of prominent Bragg peaks at specific  $2\theta$  angles confirmed the perfect crystalline nature.

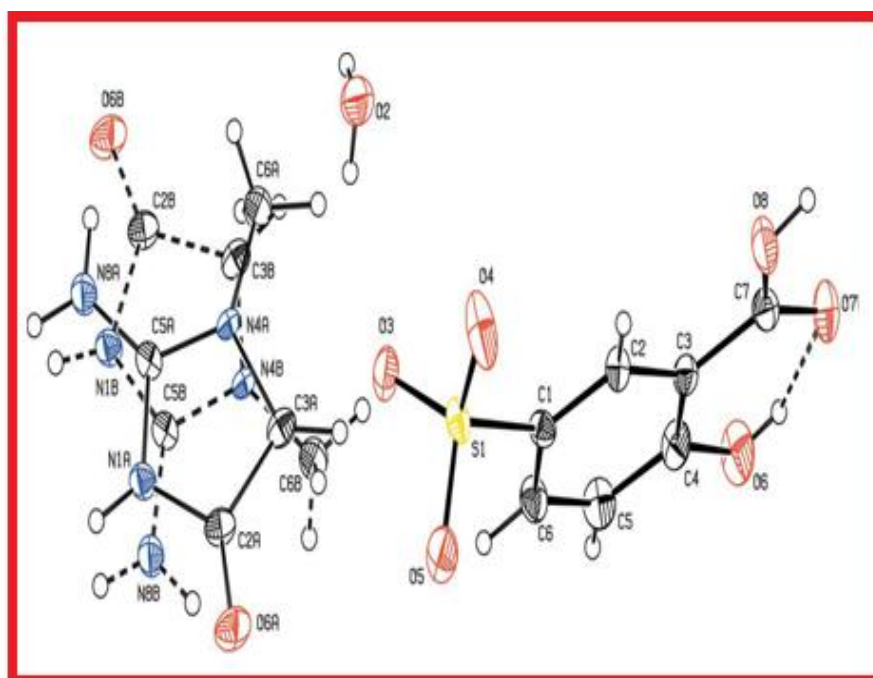


**Fig.5.4 Molecular ORTEP diagram of C5SS crystal**

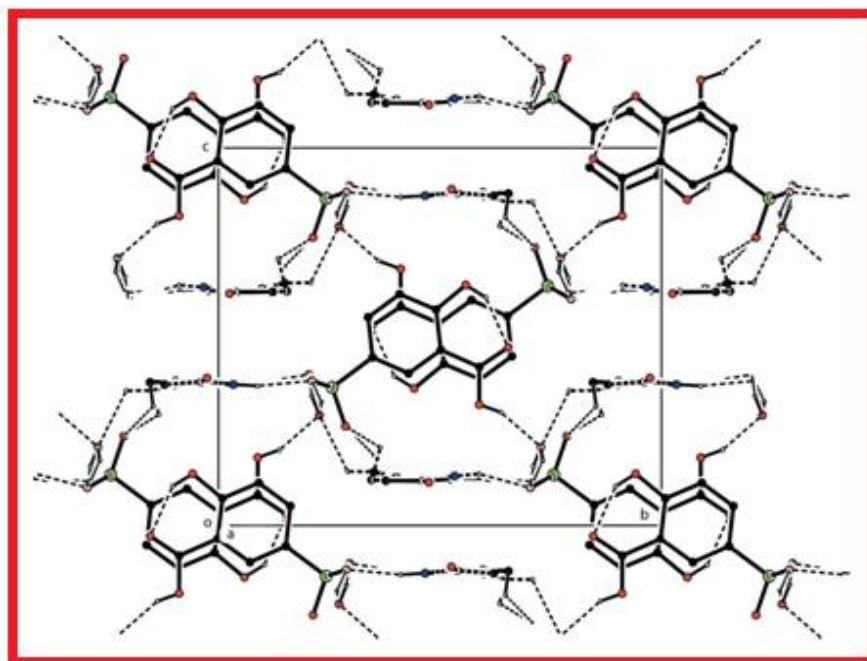


**Fig.5.5** Crystal packing diagram of C5SS viewed along ‘*b*’ axis

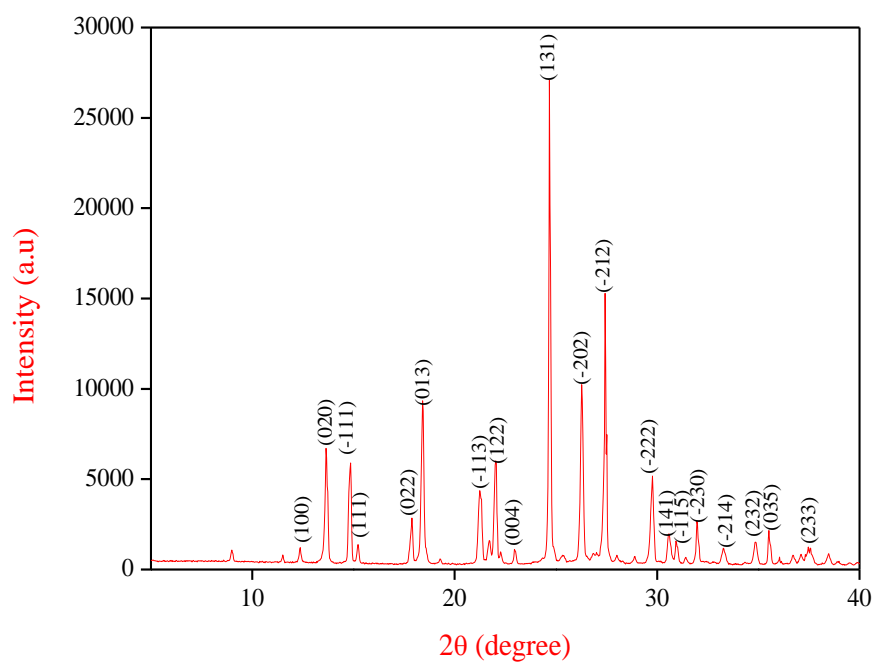


**Fig.5.6** Powder X-ray diffraction pattern of C5SS crystal

**Table 5.1 Crystal data and structure refinement for C5SS**

<b>Chemical formula</b>	<b>C<sub>4</sub>H<sub>7</sub>N<sub>3</sub>O<sup>+</sup> · C<sub>7</sub>H<sub>5</sub>O<sub>6</sub>S<sup>-</sup> · H<sub>2</sub>O</b>
M <sub>r</sub>	348.31
Crystal system, space group	Monoclinic, P2 <sub>1</sub> /c
Temperature (K)	295
a, b, c (Å)	7.2459 (2), 15.5638 (4), 13.0774 (3)
β(°)	90.100 (1)
V (Å <sup>3</sup> )	1474.79 (7)
Z	4
Radiation type	Cu Kα
μ(mm <sup>-1</sup> )	2.42
Crystal size (mm)	0.15 x 0.15x 0.10
Data collection Diffractometer Absorption correction	Bruker Kappa APEXII CCD Multi-scan (SADABS; Bruker, 2004)
T <sub>min</sub> , T <sub>max</sub>	0.587, 0.754
No. of measured, independent and observed [ <i>I</i> > 2σ( <i>I</i> )] reflections	22225, 2905, 2798
R <sub>int</sub>	0.041
(sin θ/λ) <sub>max</sub> (Å <sup>-1</sup> )	0.620
Refinement R[F <sup>2</sup> > 2σ(F <sup>2</sup> )], wR(F <sup>2</sup> ), S	0.049, 0.129, 1.09
No. of reflections	2905
No. of parameters	245
No. of restraints	2
H-atom treatment	H atoms treated by a mixture of independent and constrained refinement
Δρ <sub>max</sub> , Δρ <sub>min</sub> (e Å <sup>-3</sup> )	0.38, -0.31

**Table 5.2 Hydrogen bonds for C5SS [ $\text{\AA}$  and deg]**

<b>D-H<math>\cdots</math>A</b>	<b>D-H</b>	<b>H<math>\cdots</math>A</b>	<b>D<math>\cdots</math>A</b>	<b>D-H<math>\cdots</math>A</b>
O2-H2B $\cdots$ O3	0.82 (1)	2.13 (3)	2.799 (4)	139 (4)
O6-H6A $\cdots$ O7	0.82	1.90	2.624 (3)	146
N1A-H1A $\cdots$ O3 <sup>i</sup>	0.86	2.00	2.844 (5)	168
O2-H2A $\cdots$ O5 <sup>ii</sup>	0.82(1)	1.99(2)	2.780 (4)	161 (5)
N8A-H8AA $\cdots$ O6A <sup>ii</sup>	0.86	2.07	2.917 (5)	168
N8A-H8AB $\cdots$ O5 <sup>i</sup>	0.86	1.94	2.788 (4)	170
O8-H8 $\cdots$ O2 <sup>iii</sup>	0.82	1.85	2.616 (3)	155
C6A-H6AB $\cdots$ O4 <sup>iv</sup>	0.96	2.44	3.194 (7)	135

### 5.3.2 HRXRD Studies

The crystalline perfection of the grown C5SS single crystal was analysed by HRXRD studies. The high-resolution X-ray diffraction curve was recorded for C5SS single crystal by employing a multocrystal X-ray diffractometer with MoK $\alpha$ 1 radiation (Fig.5.7). The DC contains a single peak and it indicates that the specimen is free from structural grain boundaries. The full width half maximum of the curve was found to be 19 arc sec which is somewhat more than that expected value from the plane wave theory of dynamical X-ray diffraction for an ideally perfect crystal (Betterman et al 1964). In this present investigation, the single diffraction peak with low FWHM indicates that the crystalline perfection is good.

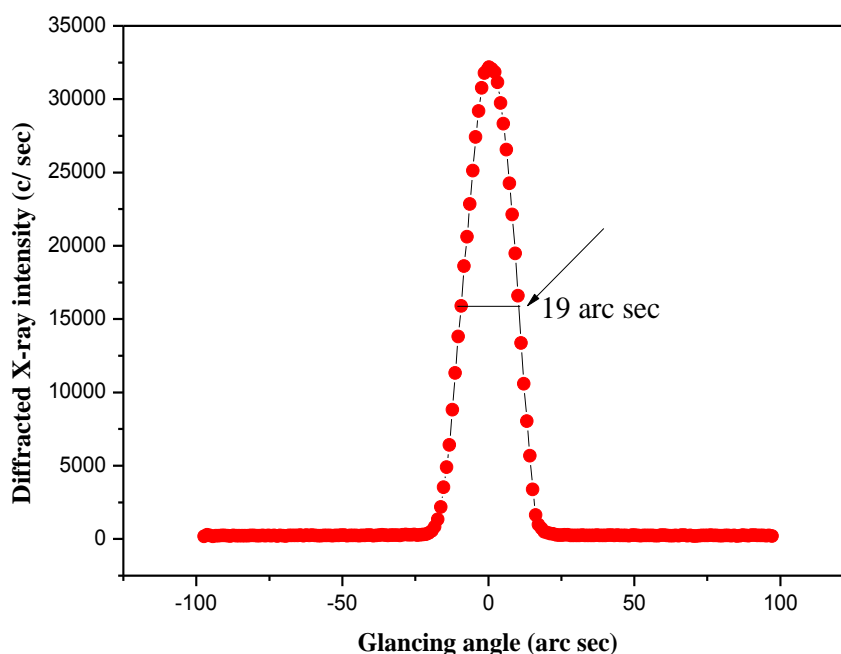


**Fig.5.7 HRXRD curve of C5SS crystal**

### 5.3.3 FTIR Spectral Analysis

The FTIR spectrum of C5SS crystal was recorded by KBr pellet technique (Fig.5.8), using Perkin Elmer FTIR spectrometer in the range 4000-400  $\text{cm}^{-1}$ . The presence of various functional groups in C5SS was identified using FTIR spectral analysis. The N-H stretching of secondary amines assigned at 2418  $\text{cm}^{-1}$  is due to the protonation of amino group foremost to the formation of C5SS compound. Asymmetric stretching of deprotonated carboxylate ions observed at 1582  $\text{cm}^{-1}$ . C=N asymmetric stretching appeared at 1498  $\text{cm}^{-1}$ . The peaks observed at 1225 and 1066  $\text{cm}^{-1}$  are due to C-N asymmetric and symmetric stretching vibrations. The peak observed at 916  $\text{cm}^{-1}$  is due to S-O asymmetric stretching vibration. The C-H out-of-plane bending vibration observed at 766  $\text{cm}^{-1}$ . The peaks

appeared at 588 and 530  $\text{cm}^{-1}$  are due to COOH wagging and  $\text{COO}^-$  wagging vibrations (Silverstine et al 2004). Table 5.3 shows the spectral assignments of C5SS compound.

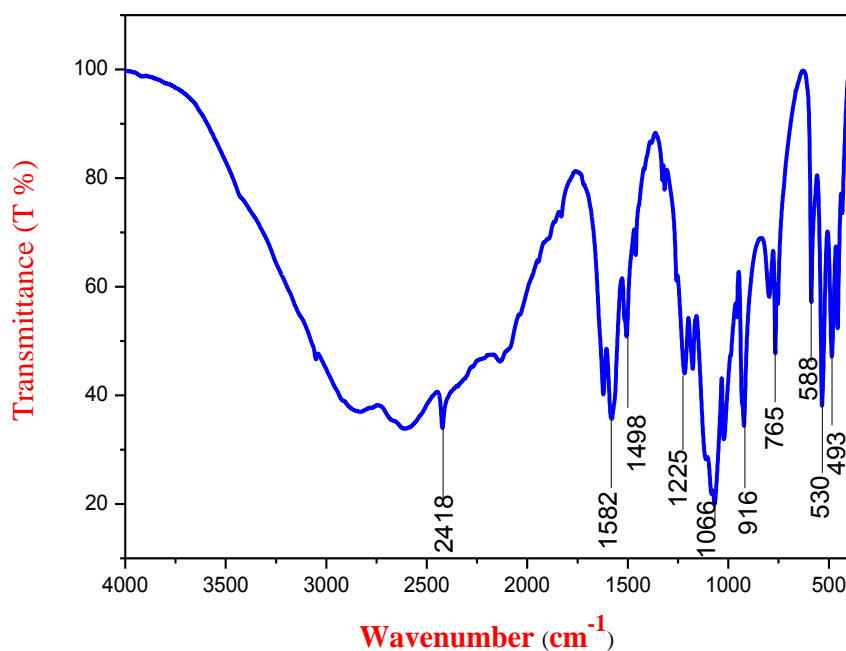


**Fig.5.8 FTIR spectrum of C5SS crystal**

**Table 5.3 FTIR molecular vibrational assignments of C5SS**

Wave number ( $\text{cm}^{-1}$ )	Assignments
2418	Stretching mode of protonated secondary amine salt
1582	Asymmetric stretching of deprotonated carboxylate ions
1498	C=N asymmetric stretching
1225, 1066	Asymmetric and symmetric stretching vibration of C-N
916	S-O asymmetric stretching
765	C-H out-of-plane bending
588	COOH wagging
530	$\text{COO}^-$ wagging

#### 5.3.4 Thermal Analysis

The thermal stability of grown C5SS crystal was confirmed by using simultaneous measurement of thermogravimetric (TG) and Differential scanning calorimetric (DSC) traces. Thermal studies of the title compound were carried out by using SII TG-DSC 6300 EXSTAR instrument in nitrogen atmosphere at a heating rate of 2°C/min. From the TGA curve (Fig.5.8), it was observed that, C5SS material has thermal stability upto 120°C and found that the decomposition of the title compound occurs in three stage weight loss originated in the range 121°C - 165°C and continued upto 222°C and third stage prolonged to 319°C. The observed weight loss is due to the liberation of volatile substances such as CO, CO<sub>2</sub> and hydrocarbons. In corresponding DSC, sharp endothermic peak noted at 137°C is due to the melting point of C5SS material. From these results, it was concluded that the C5SS crystal is capable to function upto 120°C which could be useful in optical applications.

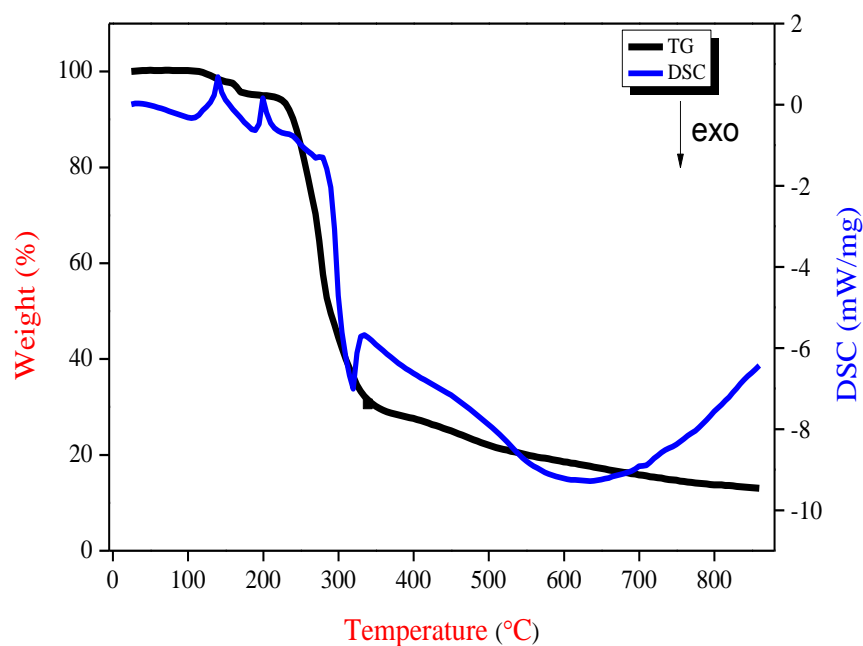


**Fig.5.9 TG-DSC thermogram of C5SS crystal**

### 5.3.5 UV –Vis Transmission Studies

The optical transmission analysis is significant to establish potential NLO materials. UV-Vis optical transmission effects give an optical network of materials essentially optical transparency gap and band gap energy which are used in linear and nonlinear utilization. Consequently, crystal is required to gain large transparency in potential electromagnetic band that depends on the use of optical applications. The optical transmission spectrum of cut and polished C5SS crystal sample of 2 mm thickness was used to record the UV-Vis transmission spectrum in the range 190-900 nm. The recorded transmission spectrum is shown in Fig.5.10. UV-visible transmission

spectrum reveals that C5SS crystal has the optical transmittance about 73% with cut-off wavelength 328 nm (ultraviolet region).

The band gap of the C5SS crystal was calculated using the Tauc's relation:  $(\alpha h\nu)^n = A(h\nu - E_g)$ , where,  $\alpha$  indicates the absorption coefficient,  $\nu$  is the incident frequency,  $h$  is the Planck's constant and  $E_g$  is the band gap energy (Tauc et al 1966). Tauc's plot drawn between  $(\alpha h\nu)^2$  and photon energy ( $h\nu$ ) is shown in Fig.5.11. From the plot, the band gap energy ( $E_g$ ) was found to be 3.7 eV.

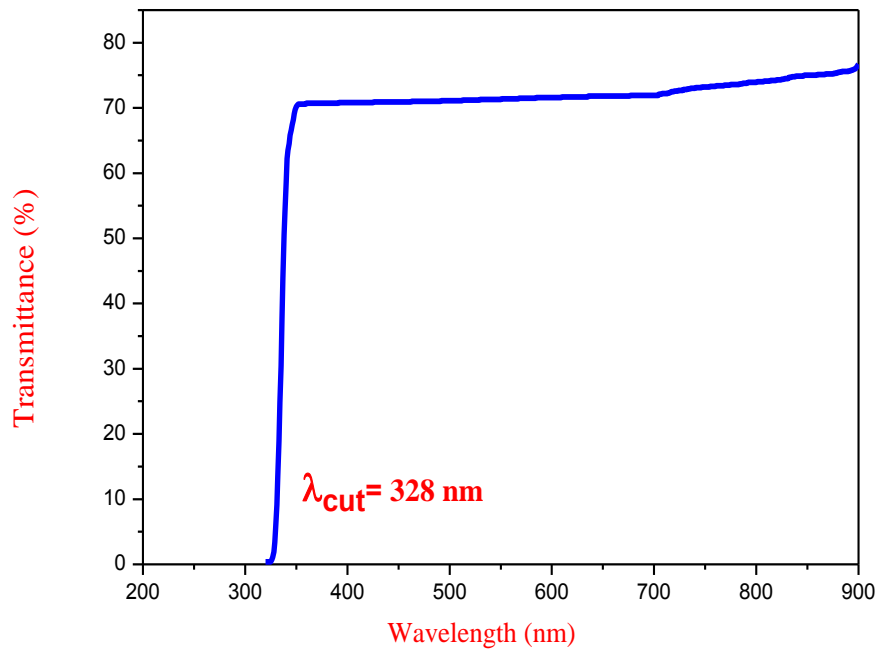


**Fig.5.10 UV-Visible transmission spectrum of C5SS crystal**

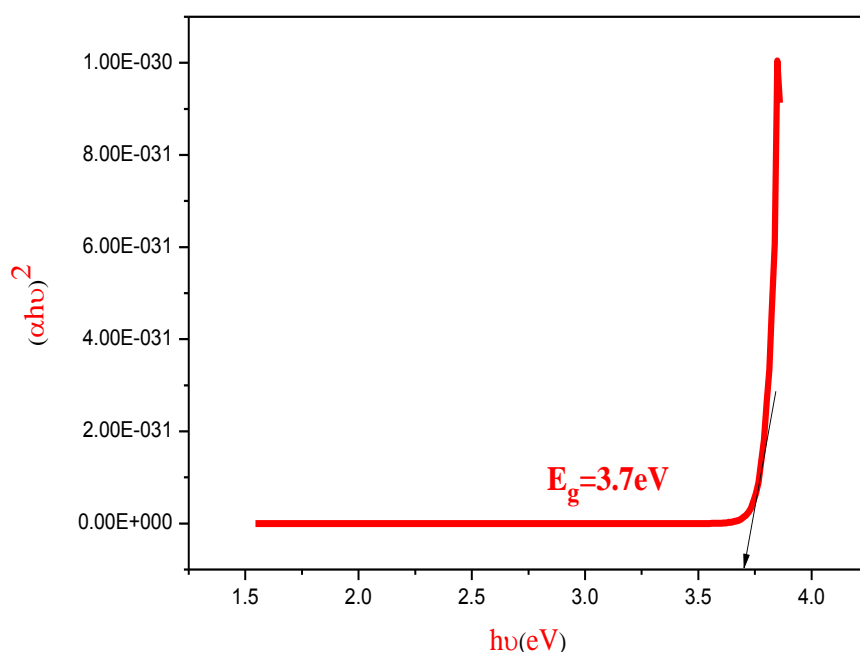


**Fig.5.11 Tauc's plot drawn between  $(\alpha h\nu)^2$  and  $h\nu$  of C5SS crystal**

### 5.3.6 Photoluminescence Studies

The photoluminescence analysis was carried out for the grown crystal using RF-5301 Spectrometer. PL spectrum of C5SS was recorded at room temperature with an excitation wavelength 328 nm. Photoluminescence (PL) intensity is predominant based on the excitation energy along with the intensity of incident beam. The study of optical properties is used for quality analysis and to estimate the crystal defects owing to the presence of foreign matter in the organic crystal as illuminated from fluorescence spectroscopy (Prabhakaran et al 2014). PL spectrum of C5SS showed a strong single emission peak at 443 nm upon with 328 nm excitation wavelength (Fig.5.12). It covered the violet region of the visible spectrum, which may be occurred

due to the  $\pi^* \rightarrow n$  transition. Since, C5SS crystal possess violet emission property, it will be useful in the fabrication of violet lasers (Dalal et al 2016).

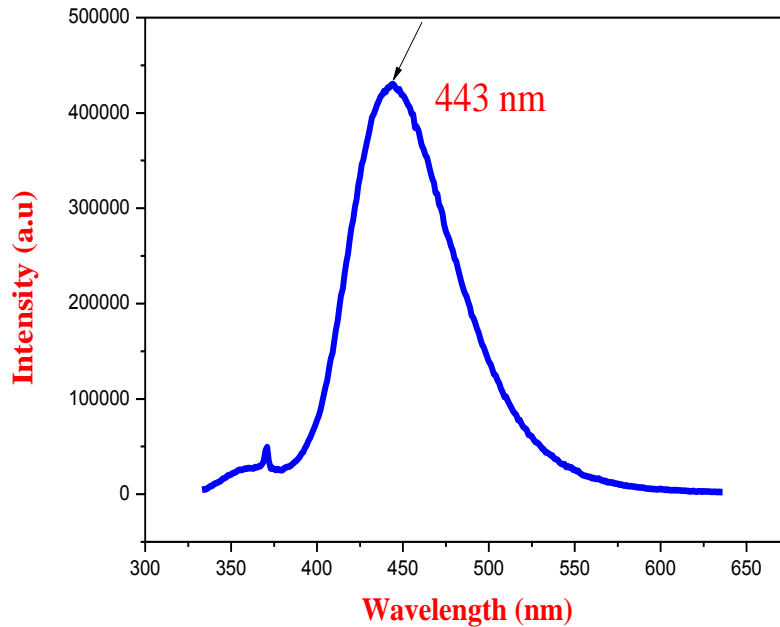


**Fig.5.12 Photoluminescence spectrum of C5SS crystal**

### **5.3.7 Laser Damage Threshold Studies**

High optical intensities are involved in the nonlinear optical applications, so that the nonlinear crystals must withstand to high power intensities. The laser damage threshold was measured by using induced high intensity laser light on 2PE5S crystal surface. A Q-switched Nd:YAG laser source of pulse width 10 ns and repetition rate of 10Hz was used. The controlled energy of laser beam produced by the variable attenuator was made to fall on the test sample located at the focus of converging lens.

The energy density of the input laser beam was recorded for which the crystal gets damaged. The LDT value was calculated using the relation,

$$\text{Power density } P_{(d)} = E/\tau A \quad (5.1)$$

The calculated laser damage threshold value of C5SS crystal is 5.23 GW/cm<sup>2</sup>, which is higher than that of KDP crystal (Vijayan et al 2006). The high value of LDT depends on the quality of the crystal. The C5SS crystal can able to use the laser damage capability level upto 5.23 GW/cm<sup>2</sup>.

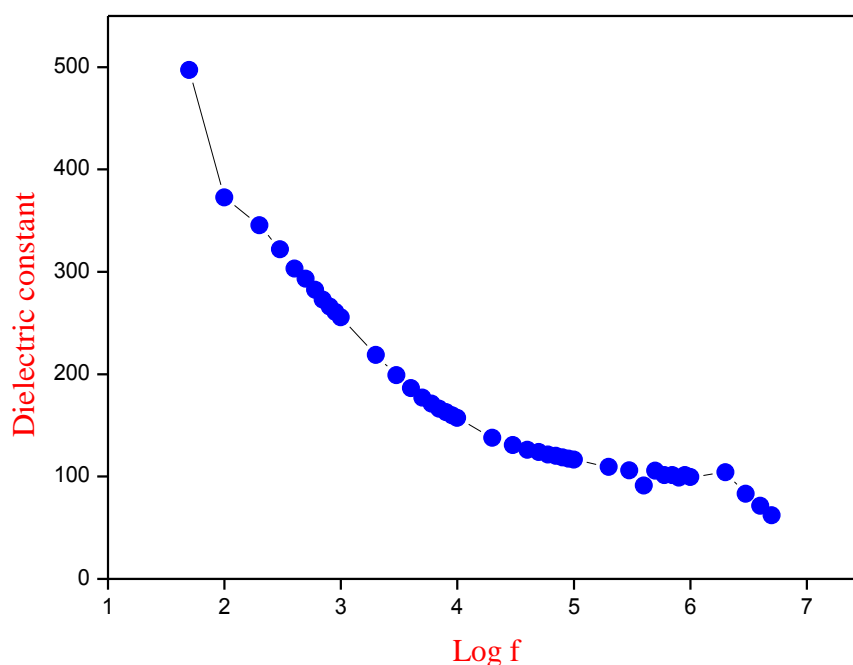
### 5.3.8 Dielectric Studies

Dielectric properties are one of the primary electro-optical properties of solids. Using HIOKI3532-50LCRHITESTER, the dielectric constant and dielectric loss of PMBS crystal have been measured in the frequency range 50 Hz–5 MHz for the temperature range 40–120 °C. A well polished crystal was subjected to dielectric measurements. The variation of dielectric constant and dielectric loss as a function of frequency at various temperatures has been analysed. The dielectric constant can be calculated using the relation,

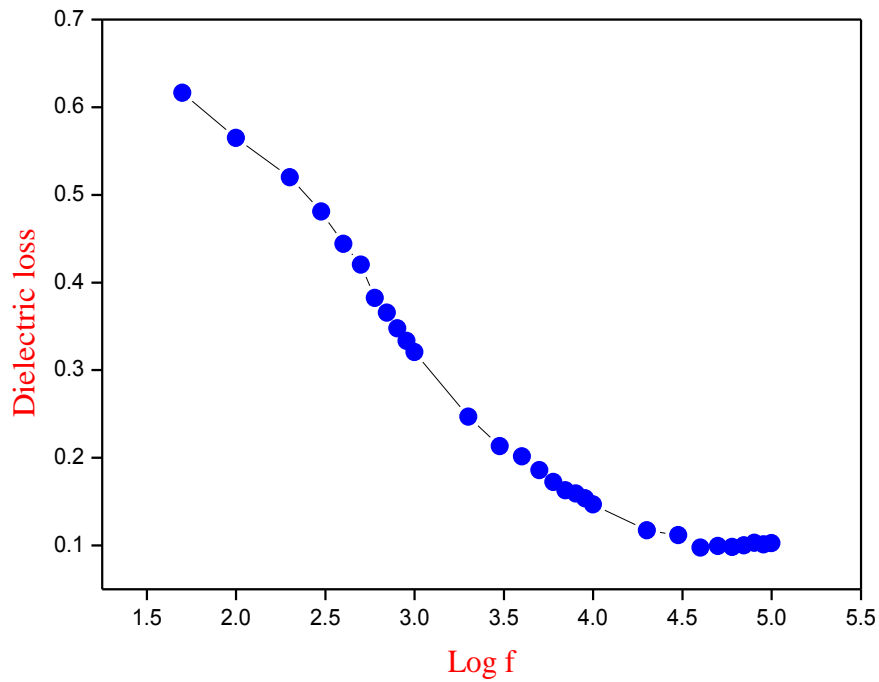
$$\epsilon_r = Ct / \epsilon_0 A \quad (5.2)$$

Figure 5.13 shows that the dielectric constant has higher value at low frequencies and nearly constant at high frequencies. The magnitude of

dielectric constant depends on the degree of polarization and space charges in crystals. Figure 5.14 shows the variation in dielectric loss ( $\tan\delta$ ) with frequency. The low dielectric loss with high frequency provides that the crystal possesses good optical quality with lesser defects (Smyth et al 1955). Therefore, the low value of dielectric constant and dielectric loss are more important for materials used in the NLO devices.



**Fig.5.13 Plot drawn between dielectric constant and log frequency of C5SS crystal**



**Fig.5.14 Plot of dielectric loss vs log frequency of C5SS crystal**

### 5.3.9 Mechanical Studies

Hardness is one of the essential mechanical properties to find the nature and strength of a material. The well polished C5SS crystal was employed on the flat surface of crystal for different loads and it continued up to the cracks formed due to the excess load, which is the indication of hardness limit of the crystal. The Vicker's hardness values were determined using the relation,

$$H_v = \frac{1.8554 P}{d^2} \quad (\text{kg/mm}^2) \quad (5.3)$$

The relation among hardness number ( $H_v$ ) and load ( $P$ ) for C5SS is shown in Figure 5.15. The hardness decreases progressively with the increase

in load (ISE). Meyer's index  $n$  was calculated from the graph (Figure 5.16) plotted against  $\log P$  versus  $\log d$ . The value of 'n' obtained for C5S5S crystal using linear fit is found to be  $n = 1.5$ . Hence, C5SS crystal was found to possess hard material category.

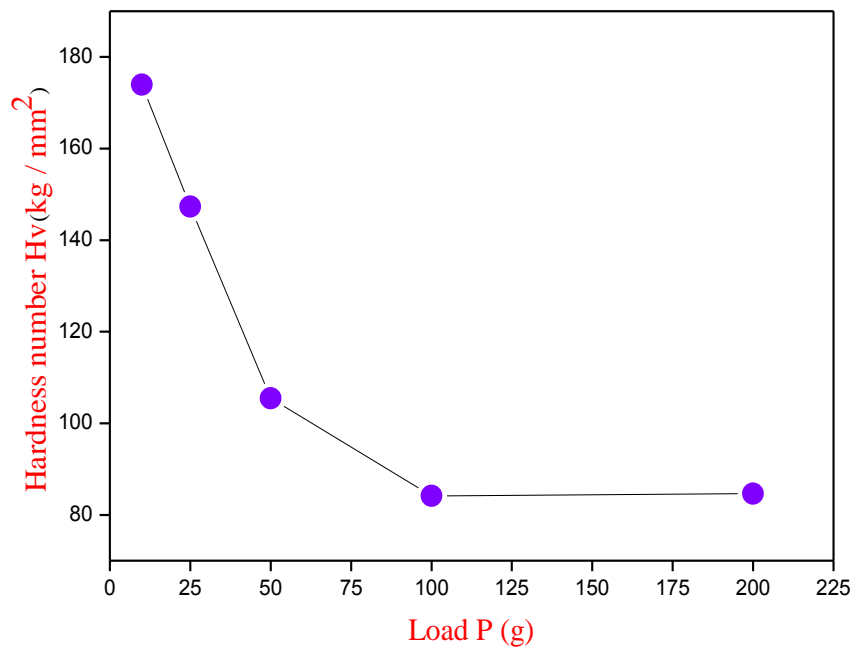


**Fig.5.15 Plot drawn between Vicker's hardness number ( $H_v$ ) and load (P) of C5SS crystal**

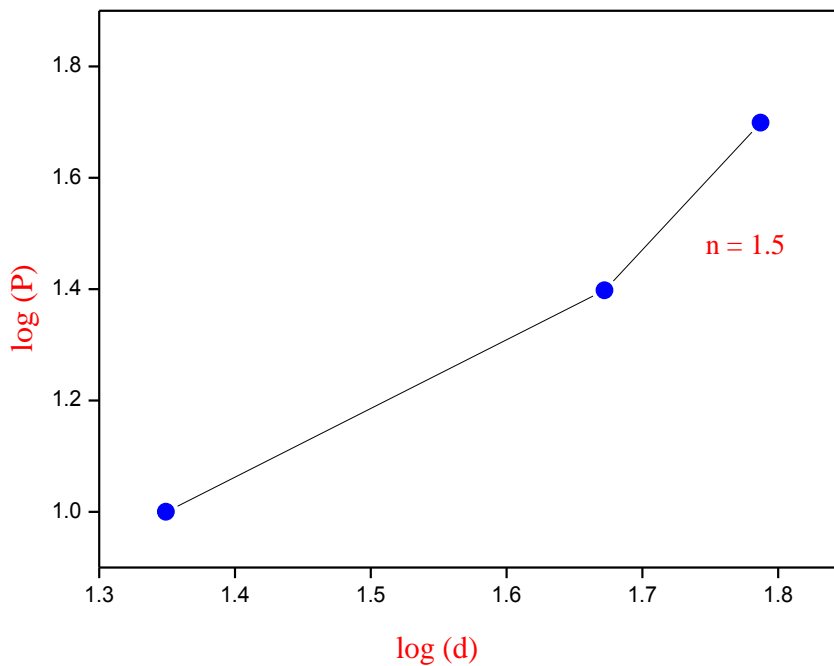


**Fig.5.16 Plot drawn between log P and log d of C5SS crystal**

### 5.3.10 Third Order Nonlinear Optical Studies

By using Z-scan technique, the third-order nonlinear optical property of C5SS crystal was studied. Based on the Z-scan data measured in open and closed aperture modes, the nonlinear refractive index ( $n_2$ ), nonlinear absorption coefficient ( $\beta$ ) and nonlinear optical susceptibility ( $\chi^3$ ) of the grown crystal were estimated. In this experiment, an optically polished crystal sample was used for molecular excitation and its propagation direction has been taken in the Z-axis. The beam was focused by using a convex lens of focal length 22.5 cm and the focal point was taken as  $Z=0$ . The normalized transmission from the crystal was measured by placing the crystal sample in different positions with respect to the focus of the beam.

From the normalized transmission of Z-positioned crystal sample, the nonlinear absorption coefficient and nonlinear optical refraction were measured. The monochromatic laser light (632.8 nm) with output power 20 mW beam from He-Ne laser source was used. The optically polished 1mm thick crystal sample was fixed in the travel range of 12 mm. Using the powermeter, the input energy and the energy transmitted by the sample were measured.

The transmittance difference between the peak and valley ( $\Delta T_{p-v}$ ) can be calculated from the Z-scan data (Subashini et al 2011; Sabari Girisun et al 2011). The normalized transmittance of closed and open apertures is shown in Figs.5.17&5.18. From the experimental data, the effective third-order nonlinear refractive index ( $n_2$ ) value was found to be  $(n_2) = 9.77 \times 10^{-8} \text{ cm}^2/\text{W}$ , nonlinear absorption coefficient  $(\beta) = 0.07 \times 10^{-4} \text{ cm/W}$  were found out. The third order nonlinear optical susceptibility were estimated to be  $(\chi^{(3)}) = 11.21 \times 10^{-6} \text{ esu}$  (Sabari Girisun et al 2011; Sudharsana et al 2012).

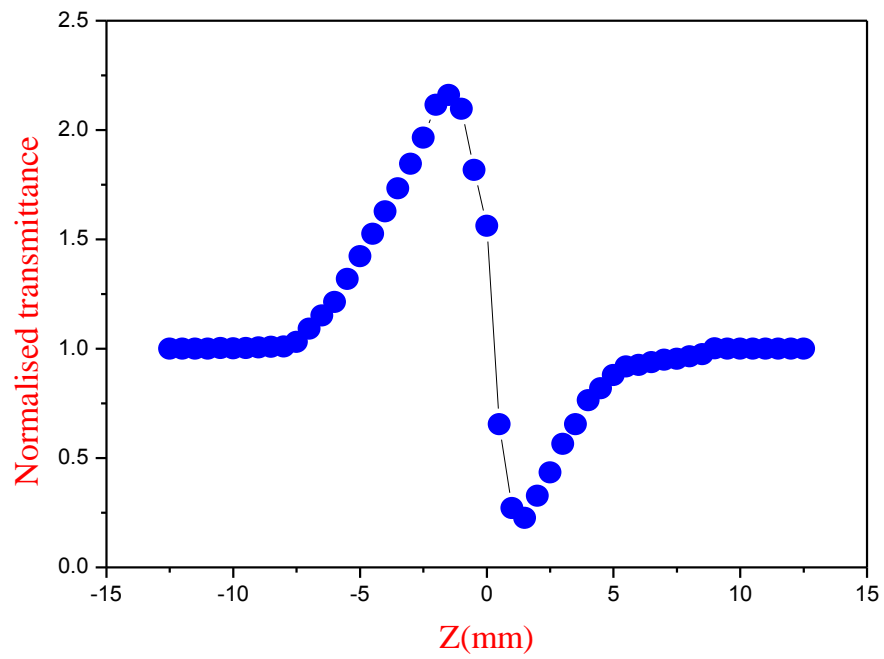


**Fig.5.17 Z-scan plot traced for C5SS crystal in closed aperture mode**

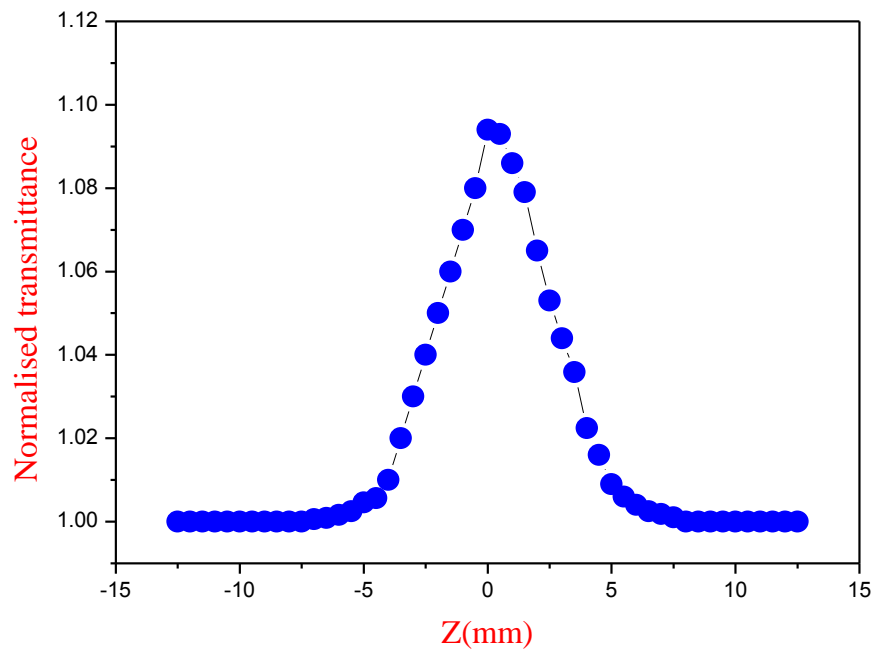


**Fig.5.18 Z-scan plot traced for C5SS crystal in open aperture mode**

**Table 5.4 Third order nonlinear optical parameters of C5SS crystal measured in Z-scan experiment**

<b>Optical Parameters</b>	<b>Values</b>
Nonlinear refractive index ( $n_2$ )	$9.77 \times 10^{-8} \text{ c m}^2/\text{W}$
Nonlinear absorption coefficient ( $\beta$ )	$0.07 \times 10^{-4} \text{ cm/W}$
Third-order nonlinear optical susceptibility ( $\chi^{(3)}$ )	$11.21 \times 10^{-6} \text{ esu}$
Second order hyperpolarizability ( $\gamma_h$ )	$3.817 \times 10^{-6} \text{ esu}$

#### **5.4 CONCLUSION**

Creatininium 5-sulfosalicylate nonlinear optical crystal was grown by slow evaporation solution growth method. X-ray diffraction analysis revealed the unit cell parameters and crystalline perfection.

FTIR spectral analysis revealed the vibrational behaviour of the synthesized compound and confirmed its necessary functional groups. From thermal analysis, the melting point (161°C) and decomposition states of grown crystal were observed. UV-Vis transmittance study revealed the transparency, cut-off wavelength and band gap energy of title crystal.

Luminescence spectrum of grown C5SS crystal showed the violet fluorescence light. The laser damage threshold of grown C5SS crystal was found to be  $5.23 \text{ GW/cm}^2$ . The nonlinear refractive index, nonlinear absorption and third-order nonlinear optical susceptibility were estimated by Z-scan technique.